EVAPORATION-DETERMINED MODEL FOR ARC HEAT INPUT IN THE CATHODE AREA BY GMA WELDING

O. MOKROV*, M. SIMON*, A. SCHIEBAHN* and U. REISGEN*

**RWTH Aachen University, ISF – Welding and Joining Institute, 52062 Aachen, Germany, simon@isf.rwth-aachen.de*

DOI 10.3217/978-3-85125-615-4-50

ABSTRACT

The most used approaches for the modelling of the heat input in GMA welding process simulation usually assume an axisymmetrical Gaussian distributed heat flux in the cathode region, whereas it has been suggested that the attachment region of the arc to the cathode consists of several highly mobile elemental cathode spots. It is assumed, that the processes in each mobile spot are not stable, but are strongly influenced by the evaporation from the workpiece. Their existence is therefore transient and outside of equilibrium. To calculate the heat input in this area, a concept has been developed on the basis of a cellular automaton method, which allows to calculate the resulting heat flux distribution. At the core of this concept is a simplified model for the elementary cathode spot, which delivers the heat flux and the current density, while taking into account effects of evaporation, which are characteristic for the real GMA welding process.

The cellular automaton consists of a grid, whose size is related to the typical size of the cathode spot, taken from literature. The random motion of the spots is simulated according to a probability distribution, which is dependent on the potential heat release of each cathode spot to the cathode surface and therefore also the cathode surface temperature. The number of spots is counted to satisfy a „fuzzy“ current continuity. Additionally a condition is implemented to take into account the state of the arc area.

In a next step this model will be coupled to a weld pool calculation.

Keywords: GMA, cathode, evaporation, heat flux, current density

INTRODUCTION

The gas metal arc welding (GMAW) is used widely in the industry due to its high reliability and productivity. However, as it is a complex phenomenon involving many interacting physical mechanisms, the development of the understanding of the process in detail is still ongoing. To further this understanding, the method of computer simulation is increasingly used. Welding simulation can be distinguished into three areas, following Radaj [1], and this work is concerned with a part of process simulation, where the accurate prediction of shape and size of the weld pool, according to the welding process parameters, is attempted. The phenomena that need to be taken into account include the resistance of the cables and the wire electrode, the droplet formation and detachment, the arc including heat transfer,

melting and solidification enthalpies and heat conduction within the work piece. For the magneto-hydrodynamic calculation of the weld pool the most sensitive boundary condition is that of the cathode layer, together with the effects of the heated molten droplets. In the recent works [2], [3], the cathodic heat flux is treated as a fixed Gaussian function, following [4], however in this work a model is presented to determine a new distribution.

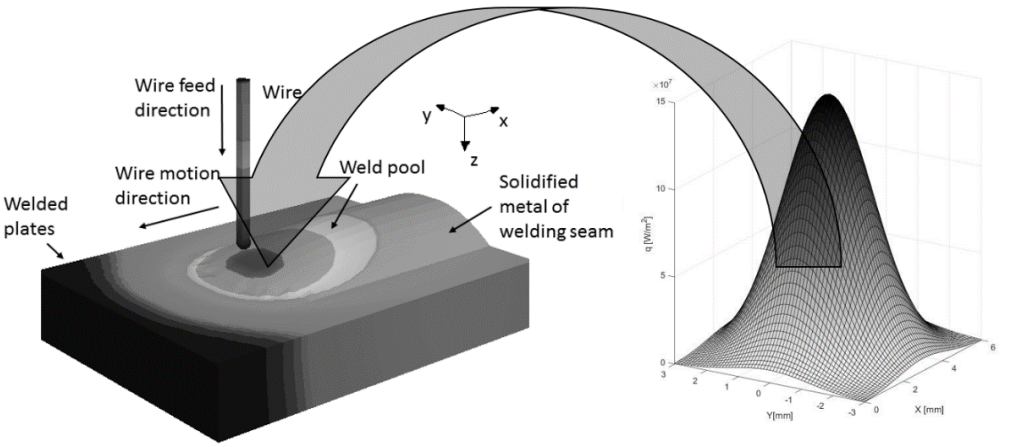

Fig. 1 Gaussian distribution, as usually used as cathode heat source in GMA weld pool calculation.

PROBLEM STATEMENT

It has been observed that the cathode region in an arc discharge consists of multiple highly mobile cathode spots (CS) on the weld pool [5]. The exact dynamic of the CS have so far remained unclear due to their very small spatio-temporal dimensions and the descirption of their properties still represents a field of active research. On a solid cathode, it is observed, that in an absence of an external magnetic field the spots seem to follow a quasi-stochastic random walk [6], which justifies the assumption of a Gaussian distribution (Figure 1) as a fair first approach. However it has been shown in experiments, that the CS follow a different distribution on a molten cathode [7], where it seems like they tend to avoid the center, where the hottest temperatures occur. In the present work, the authors present a concept to relate the cathode spot probability to the cathode surface temperature, by an evaporation-dependent model for the heat flux of the elementary cathode spot. In a second step this model will be used to calculate new heat flux and current density distributions which can be considered to be dependent on evaporation. The model of the elementary cathode spot is based on descriptions of the cathode layer found in the literature, although it uses an original approach to describe the ion current density, assuming a non-linear ionization process which is treated as a black box. This allows to match the current density to the empirically observed high current densities on non-refractory materials, which cannot be explained by thermionic emission, as is the case in refractory materials like tungsten. Additionally it assumes a strong damping effect to the ion current density, due to evaporation.

MODEL DESCRIPTION

MODEL OF ELEMENTARY CATHODE SPOT

The main phenomena which were considered to contribute to the net heat flux are the following: Heat gains by ion bombardment q_{ion} and back diffused electrons q_{ebd} and heat losses by thermionic emission q_{em}, evaporation q_{evap}, heat conduction q_{cond} and radiation q_{rad}. In order to calculate these, the current densities of thermionic electrons, ions and back-diffused electrons need to be known.

$$q_{CS} = q_{cond} = q_{ion} + q_{ebd} - q_{evap} - q_{em} - q_{rad} \tag{1}$$

The external parameters for the Model were $d_{Sheath} = 10^{-8}$ m; $U_D = 10$ V, the thickness of the cathode sheath and the voltage drop, according to [8]. The heavy particle temperature T_h is assumed to equal the surface temperature of the wall T_w due to thermalization with evaporated atoms.

$$T_h = T_w \tag{2}$$

The electron temperature in the plasma is estimated by

$$T_e = \frac{(e \cdot U_D + k_B \cdot T_W - e \cdot E_{ion})}{3/2 \cdot k_B} \tag{3}$$

with k_B Boltzmann constant, e electron charge and $E_{ion} = 7.9$ eV ionization energy of iron vapor.

The effective work function was taken as

$$A_{eff} = A - \Delta A \tag{4}$$

with $A = 4.5$ eV being the work function for iron and

$$\Delta A = \sqrt{\frac{e \cdot U_D}{4\pi\varepsilon_0 d_{Sheath}}} \tag{5}$$

the lowering of the work function [9], with ε_0 the vacuum permittivity.

The thermionic electron current is calculated according to the Richardson-Schottky relation [10]

$$j_{em} = e\frac{4\pi k_B^2 m_e}{h^3} T_w^2 \cdot exp\left(-\frac{A - \Delta A}{k_B T_w}\right) \tag{6}$$

with m_e electron mass, h Planck constant. The ion current is calculated as

$$j_{ion} = \left(j_{em} \cdot \ exp\left(-\frac{P_{vap}^2}{P_{atm}^2} \right) \right)^{1.6} \tag{7}$$

The exponent of 1.6 is chosen to match the total current density found by Meysats [11] of $j_{CS} = 1 - 3 \cdot 10^{12}\ \mathrm{A/m^2}$, with P_{vap} the pressure of vaporized material Eqn. (7) taken from [12], P_{atm} the atmospheric pressure, $T_b = 3134\ \mathrm{K}$ the boiling temperature of iron, $H_{vap} = 347 \cdot 10^3\ \left[\frac{J}{mol}\right]$ the molar heat of vaporization of iron and R the gas constant.

$$\mathrm{P_{vap}} = \mathrm{P_{atm}} \cdot \exp\left[\frac{-\mathrm{H_{vap}}}{\mathrm{R}} \left(\frac{1}{\mathrm{T_W}} - \frac{1}{\mathrm{T_b}} \right) \right] \tag{8}$$

The back-diffused current is estimated as

$$j_{ebd} = (j_{em} + j_{ion})/2 \cdot exp\left(-\frac{eU_D}{kT_e} \right) \tag{9}$$

The total current is therefore given as

$$j_{CS} = 2j_{ion} - j_{ebd} + j_{em} \tag{10}$$

The corresponding heat fluxes are given as

$$\begin{aligned} q_{ion} &= \frac{j_{ion}}{e} \left[\mathrm{k_B} \left(2T_h + \frac{ZT_e}{2} - 2T_W \right) + \ \mathrm{ZeU_D} + \ + \mathrm{E_{ion}} - \mathrm{ZA_{eff}} \right] \\ &\approx \ \frac{\mathrm{j_{ion}}}{\mathrm{e}} \left[\mathrm{k_B} \frac{\mathrm{T_e}}{2} + \mathrm{eU_D} + \mathrm{E_{ion}} - \mathrm{A_{eff}} \right] \end{aligned} \tag{11}$$

following [8], with Z=1, considering only the first ionization for simplification.

$$q_{ebd} = \frac{j_{ebd}}{e} (2kT_e + A_{eff}) \tag{12}$$

according to [8].

$$q_{em} = \frac{j_{em}}{e} (2kT_W + A_{eff}) \tag{13}$$

according to [8].

$$q_{evap} = J_{vap} H_{vap} / M_{iron} \tag{14}$$

following [12], with M_{iron} the molar mass of iron and

$$J_{vap} = \left(\frac{m_M}{2\pi k_B T_w}\right)^{1/2} P_{vap} \tag{15}$$

the flux of evaporated particles in diffusive mode according to [13].

$$q_{rad} = \varepsilon\sigma T_w^4 \tag{16}$$

according to [14], with $\varepsilon\sigma = 5.670367 \cdot 10^8\ \mathrm{J/(s \cdot m^2 \cdot K^4)}$ the Stefan-Boltzmann constant.

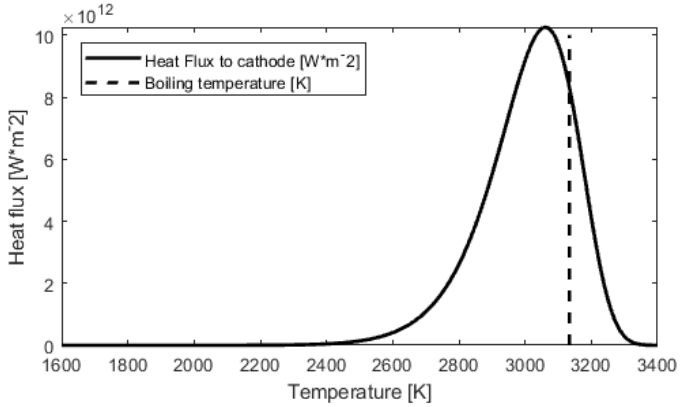

Fig. 2 Dependence of heat flux on surface temperature.

The proposed model states a relationship between the surface temperature and the expected heat flux as well as the current density in case of a cathode spot, see Figure 2 and Figure 3.

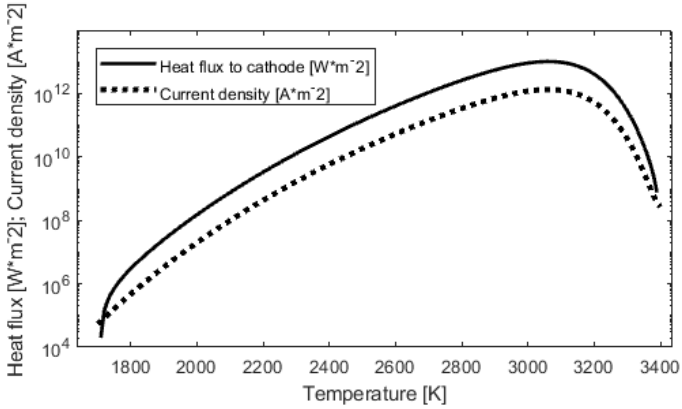

Fig. 3 Dependence of heat flux and current density on surface temperature in logarithmic scale.

MODEL OF CATHODE SPOT DISTRIBUTION

Assuming a initial temperature field $T_{0;w}(x, y)$ (Figure 4) of a fully developed weld pool surface, a new distribution of CS is selected by sampling locations of single CS without replacement according to a probability $P(x, y)$. The probability at each location is chosen

to be directly proportional to the possibly generated heat flux, convoluted with a Super-Gauss function to take into account the influence of distance of the anode tip to the cathode, favoring a spot close to the center below the torch (x_0, y_0), with $r_x = 3 \cdot 10^{-3}$ m, $r_y = 3 \cdot 10^{-3}$ m, $x_0 = 3 \cdot 10^{-3}$ m and $y_0 = 0 \cdot 10^{-3}$m. Here $k = 3/(r_x r_y)$ is a geometrical parameter, which influences the spreading, similar to a standard deviation.

$$P_{abs}(x,y) = q_{spot}\left(T_w(x,y)\right) \cdot \exp\left(-\left(k((x-x_0)^2 + (y-y_0)^2)\right)^2\right) \quad (17)$$

$$P(x,y) = \frac{P_{abs}(x,y)}{\int P_{abs}(x,y)dxdy} \quad (18)$$

The grid size is chosen according to the assumed diameter of the CS of $\Delta x = 5$ µm and the time step is chosen as $\Delta t = 5 \cdot 10^{-8}$ s following [10] and [5], giving an approximate speed of the CS of $v_{CS} = 10^2$ m/s.

Initially a number of CS is generated on the grid, until the total current surpasses a fixed value $I = 180$ A. If the total current is higher than the fixed value of I, the number of CS will be reduced in the next time step, picking according to the inverse probability inherent to each CS, until the total current falls below the fixed value again, and so on, therefore satisfying a "fuzzy" current continuity condition.

If the spot is not removed it will move around the grid in the next time step in random direction, only taking into account the probability at its adjacent fields, which is convoluted with a small Gaussian again to take into account the longer distance to diagonal grid-cells $f_{diagonal} = 0.0751$, $f_{straight} = 0.1238$.

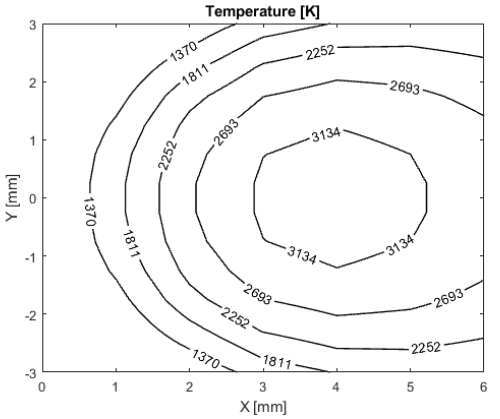

Fig. 4 Initial temperature field.

At each location where a spot resides (x_{CS}, y_{CS}) the local temperature modification of the surface is treated in a very simplified way. A local temperature gain $\Delta T(x,y,t)$ is added to the surface temperature field $T_w(x,y)$ according to a strongly simplifying assumption of transient heat transfer of a point explosion in a homogenous semi-infinite solid.

$$\Delta T(x,y,t) = \frac{H_0(t)}{(4\pi\alpha t)^{3/2}\rho C_p} \cdot exp\left(-\frac{(x-x_{CS})^2}{4\alpha t} - \frac{(y-y_{CS})^2}{4\alpha t}\right) \quad (19)$$

where H_0 is the amount of energy, $\alpha = \kappa\rho C_p$ the thermal diffusivity, κ the thermal conductivity, ρ the density and C_p the heat capacity, taken from [15], not taking into account the actual local temperature, but assuming a fixed temperature of $T_\alpha = 2450$ K everywhere.

For the calculation of H_0 also strong simplifications were applied. To save calculation time, a fixed heat flux of $q_0 = 10^{13}$ W/m^2 was assumed to act for the duration Δt. However, substantial energy losses due to evaporation were calculated according to Eq. (7), Eqn. (13) and Eqn. (14) with $T = 2450\,\text{K} + \Delta T(x, y, t_{local})$ and substracted at a local timestep of $\Delta t_{local} = 10^{-9}$ s, until the center of $\Delta T(x, y, t_{local})$ reached 10 K, after $t_{H_0;max} = 777 \cdot \Delta t$.

$$\begin{aligned} &\text{for } t < \Delta t: \\ &H_0(t) = \int (q_0 \Delta x^2 - q_{evap}(T)\Delta x^2)dt \\ &\text{for } t \geq \Delta t: \\ &H_0(t) = H_0(\Delta t) - \int q_{evap}(T)\Delta x^2 t^{0.2} dt \end{aligned} \tag{20}$$

The factor $t^{0.2}$ was added to approximate the spreading of the area of the overheated surface and was chosen as the maximum value that would still allow a numerically stable solution, however this value would depend on the used time step. The amount of energy lost due to this additional evaporation accounts for approximately 20% of the input energy $q_0 \Delta x^2 \Delta t$. The final changes remained in $T_w(x, y) = T_{0;w}(x, y) + \Delta T\left(x, y, t_{H_0;max}\right)$. In spatial direction, the additional temperature distribution $\Delta T(x, y, t)$ was limited to $29 \cdot \Delta x$ in x-direction and $29 \cdot \Delta y$ in y-direction, in order to account for the spreading of the local temperature profile after the maximum time $t_{H_0;max}$. After each time step, the new probabilities from Eqn. (17) and Eqn. (18) were calculated according to the new $T_w(x, y)$.

A schematic of the algorithm is presented in Figure 5.

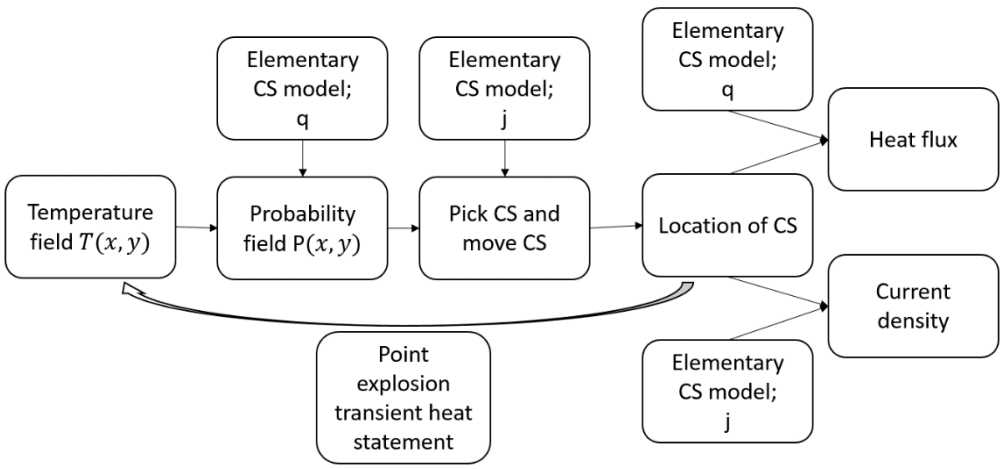

Fig. 5 Schematic of the algorithm.

RESULTS

The combined model yields several statements about the simulated cathodic arc attachment in GMA welding.

After a calculation time of 76 h 10^5 iterations have been processed, therefore a simulation time of $5 \cdot 10^{-3}$ s has been calculated. The total average current was $I = 181.3$ A. The total electrical power was $P = I \cdot U_D = 1.813$ kW, from that a total of $P_{Heat} = 1.358$ kW have been transferred to the cathode, not accounting for the 20% losses from Eqn. (20).

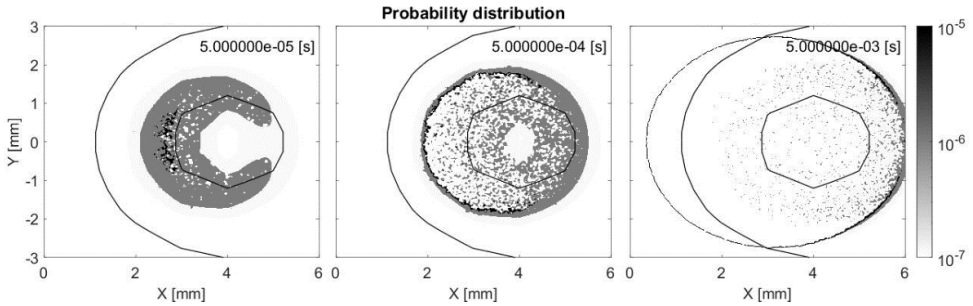

Fig. 6 Resulting probability distribution, for time $5 \cdot 10^{-2}$, $5 \cdot 10^{-1}$, 5 ms. The isolines of the liquidus and boiling temperature are overlaid.

Figure 6 presents the evolution of the probability distribution. It becomes apparent that the cathode spots modify the probability distribution locally, resulting in a very high concentration of the probability on a fine line at the front towards the welding direction.

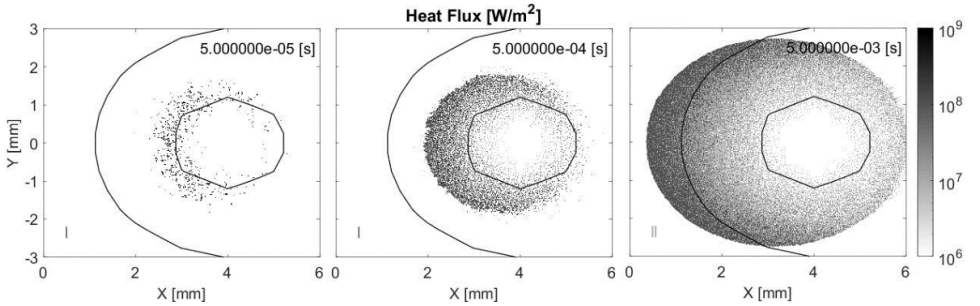

Fig. 7 Resulting heat flux distribution, for time $5 \cdot 10^{-2}$, $5 \cdot 10^{-1}$, 5 ms. The isolines of the liquidus and boiling temperature are overlaid, as well as an indication for the distance traveled by the torch in the lower left corner.

In Figure 7 the resulting heat flux distribution is presented. The welding direction is from right to left. It becomes apparent, that a sickle shape of the heat flux distribution is present with an emphasis towards the melting front. As the movement of the torch has not been taken into account, an arrow was placed in the figures (lower left) to indicate the movement of the plate according to time-scale and grid resolution, assuming a welding speed of 80 cm/min. The distance traveled by the torch after 5 ms equals $d = 6.67 \cdot 10^{-4}$m.

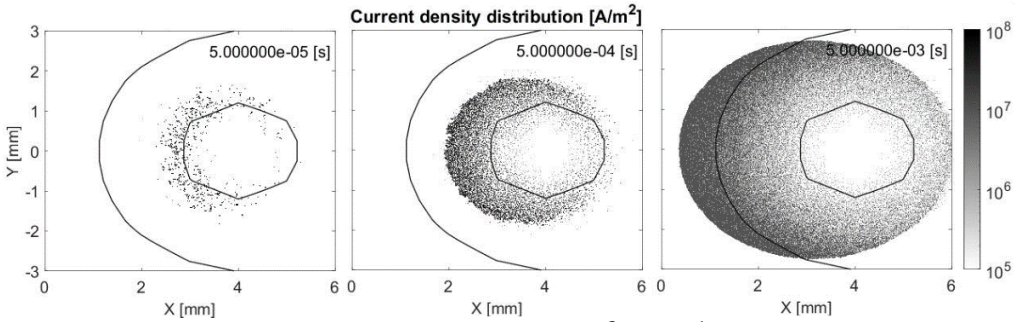

Fig. 8 Resulting heat flux distribution, for time $5 \cdot 10^{-2}$, $5 \cdot 10^{-1}$, 5 ms. The isolines of the liquidus and boiling temperature are overlaid.

As the distribution reflects the locations of the CS, the distribution of the current density in Figures 8 follow the distribution of the heat flux, however with values about one order of magnitude lower, as expected from the model (Figure 3).

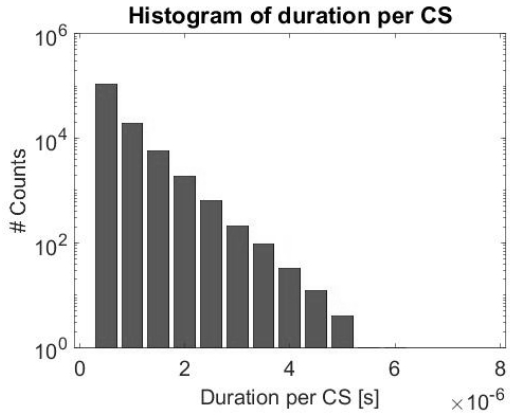

Fig. 9 Semi-logarithmic histogram of the duration of a CS in intervals of $50 \cdot 10^{-8}[s]$.

Besides this, the combined model also allows some statistical statements about the duration of a CS (Figure 9) as well as the current per CS (Figure 10). Single the cathode spots lasted up to $6 \cdot 10^{-6}$ s after $5 \cdot 10^{-3}$ s simulated time. In Figure 10 it can be seen, that the substantial part of the cathode spots carry a current of more than $6 \cdot 10^{-3}$ A, which is lower than the stated possible minimum of current per cathode spot 0.1 A in [16]. The maximum current per CS was $\mathrm{I}_{\mathrm{CS,max}} = 33.4$ A.

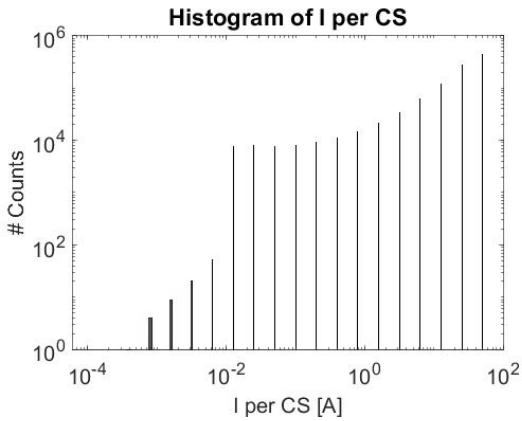

Fig. 10 Logarithmic histogram of current *I* per CS.

DISCUSSION

The presented model allows the calculation of new cathodic heat flux (Figure 7) and current density distributions to replace the widely used Gaussian approximation (Figure 1), taking into account evaporation. However, there are several drawbacks, which need to be addressed.

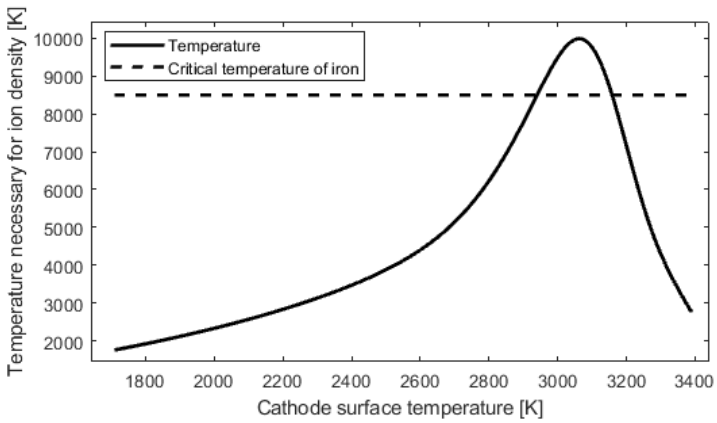

Fig. 11 Relationship between surface temperature and temperature necessary to bring forward evaporation pressure to generate the required ion densities.

The ionic current density generation is still treated as a black box and calibrated to match a semi-empirical value found for the vacuum arc. Also the presence of oxides is not considered. It should be also noted that the necessary for the ion density is much higher than the pressure generated by evaporation at that temperature (Figure 11). However, even though it seems unphysical, the cause might be found in the micro-dynamics of the CS.

Another weakness lies in the model for cathode spot distribution, as the heat transfer statement is very simplified. It assumes only an analytical expression of thermal point explosions in an isothermal, semi-infinite half space with a fixed heat flux and an additional

losses, at each cathode spot location. However, this flaw is not critical and can be overcome, even if it would slow down the calculation by a considerable amount. However, as a first approach the feasibility and structure of such model could be shown.

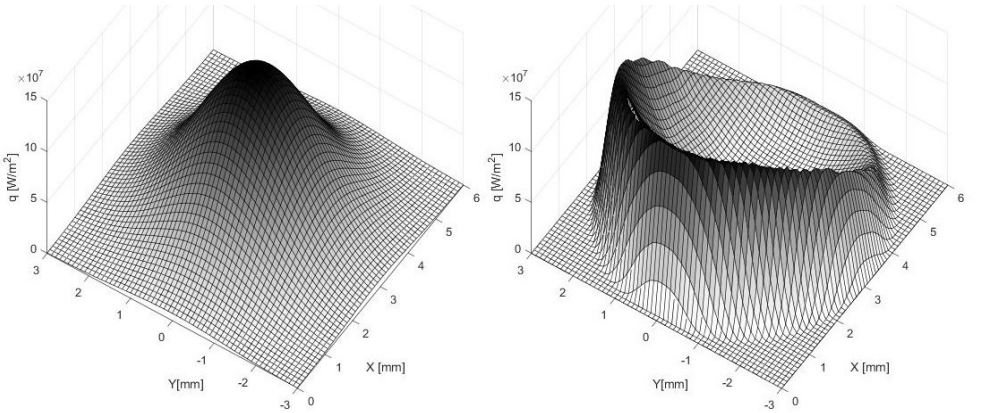

Fig. 12 Comparison between Gaussian distribution with $P = 1.358\,\mathrm{kW}$, and new resulting heat flux distribution, for time $5\,\mathrm{ms}$ as a smoothed, interpolated 3D- surface.

Another uncertainty lies in the Gauss-function, which is multiplied with the heat flux to give the local probability of the CS in Eqn. (17). As the arc pressure suppresses the liquid, and as the droplet-transfer process also has an influence on the shape of the surface, there could be effects by the electric field that have not been taken into account. In addition, the influence of the arc plasma has been neglected as well. However, it is assumed that the displayed tendencies of the distribution might be modified but not suppressed. It can be followed from the new distribution that, since the electric field within the arc column is mostly axisymmetric and concentrated at the center in the metal vapor core, a strong change of direction of the field lines must occur at the cathode, causing great deviations of Lorentz-force, which will have a strong influence on the weld pool hydrodynamics.

The hypothesis, that the cathode area in GMA welding should be treated as highly dependent on evaporation has been thoroughly studied and a novel model for the distribution of heat flux and current density has been suggested. Although there are still some open questions, the suggested model represents a continued development of the assumption of an axisymmetric Gaussian distribution and the results have been successfully used in a fast, near real-time calculation of the weld seam, in a strongly reduced form.

ACKNOWLEDGEMENT

This work was carried out with the financial support of the Collaborative Research Centre SFB1120 (DFG (Deutsche Forschungs-gemeinschaft), Sonderforschungsbereich) "Precision Melt Engineering" at RWTH Aachen University and the K-Projekt of Excellence for Metal JOINing. The K-Project Network of Excellence for Metal JOINing is fostered in the frame of COMET - Competence Centers for Excellent Technologies by BMWFW, BMVIT, FFG, Land Oberösterreich, Land Steiermark, Land Tirol and SFG. The

programme COMET is handled by FFG. For the sponsorship and the support, we wish to express our sincere gratitude.

REFERENCES

[1] D. RADAJ: *Schweissprozesssimulation – Grundlagen und Anwendung*, DVS-VERL., DÜSSELDORF, 1999.
[2] M.H. CHO ET AL.: *Simulation of Weld Pool Dynamics in the Stationary Pulsed Gas Metal Arc Welding Process and Final Weld Shape. Welding Journal supplement*. 12:271S-283S, 2006.
[3] M.H. CHO ET AL.: *Simulations of weld pool dynamics in V-groove GTA AND GMA WELDING*. WELD WORLD. 57:223-233, 2013.
[4] N. RYKALIN: *Berechnung der Wärmevorgänge beim Schweißen*. VEB Verlag Technik, Berlin, 1957.
[5] B. JÜTTNER: *Cathode spots of electric arcs.* Journal of Physics D: Applied Physics, 34:R103-R123, 2001.
[6] E. HANTZSCHE ET AL.: *On the random walk of arc cathode spots in vacuum*. Journal of Physics D: Applied Physics, 16:L173-L179, 1983.
[7] T. YUJI ET AL.*: Observation of the Behavior of Cathode Spots in AC Tungsten Inert Gas Welding on Aluminum Plate*. Quarterly Journal of the Japan Welding Society, Vol. 33, No. 2: 135s-138s, 2015.
[8] M. S. BENILOV AND A. MAROTTA: A *model of the cathode region of atmospheric pressure arcs.* Journal of Physics D: Applied Physics, 28:1869-1882, 1995.
[9] L. PEKKER: *A Sheath Collision Model with Thermionic Electron Emission and the Schottky Correction Factor for Work Function of Wall Material,* Plasma Chemistry and Plasma Processing, 37:825-840, 2017.
[10] F. CAYLA ET AL.: *Arc/Cathode Interaction Model,* IEEE Transactions on Plasma Science, 36:1944-1954, 2008.
[11] G. A. MESYATS AND I. V. UIMANOV: *2D semiempirical model of the formation of an elementary crater on the cathode of a vacuum arc,* 27th International Symposium on Discharges and Electrical Insulation in Vacuum (ISDEIV), Suzhou, 1:1-4, 2016.
[12] A. B. MURPHY: *The effects of metal vapour in arc welding,* Journal of Physics D: Applied Physics, 43:424001 32pp, 2010.
[13] M. S. BENILOV ET AL.: *Vaporization of a solid surface in an ambient gas,* Journal of Physics D: Applied Physics., 34:1993-1999, 2001.
[14] M. S. BENILOV: *Understanding and modelling plasma–electrode interaction in high-pressure arc discharges: a review,* Journal of Physics D: Applied Physics, 41:144001 31pp, 2008.
[15] B. WILTHAN ET AL.: *Thermal Diffusivity and Thermal Conductivity of Five Different Steel Alloys in the Solid and Liquid Phases,* International Journal of Thermophysics, 36:2259–2272, 2015.
[16] A. FRIDMAN: *Plasma Chemistry,* Cambridge University Press, Cambridge 2008.